A Self-Bearing 8/6 Switched Reluctance Motor

Aino MANNINEN*, Victor MUKHERJEE**, Jenni PIPPURI*, and Kari TAMMI***

*VTT Technical Research Centre of Finland Ltd

P.O. Box 1000, 02044 VTT, Finland

E-mail: aino.manninen@vtt.fi

** Department of Electrical Engineering and Automation, Aalto University

Otakaari 5, Espoo 02150, Finland

*** Department of Mechanical Engineering, Aalto University

Otakaari 4, Espoo, 02150, Finland

Abstract

This paper describes a self-bearing 8/6 switched reluctance motor (SRM). The main challenge with such a motor is how to control both torque and radial forces. This task is particularly challenging because the double saliency of the machine type causes the characteristics of the motor to be highly nonlinear. In this paper, we first present a switching logic for the 8 stator coils. The current in the 8 phases is defined by using three current components and the rotor angle. After that, we propose a model that could be used in the closed loop control to solve the required stator currents from needed radial forces and torque. The force and torque models are based on first and second order polynomials, which are fitted to data that have been obtained by two-dimensional electromagnetic finite element analysis. In this paper we compare the performance of the analytical model with the finite element analysis data, and use the analytical model for direct open loop control. The results show that the proposed analytical model can be used to calculate the required stator currents that are needed to operate the self-bearing SRM. The models can be combined with closed loop control methods in order to properly control the machine.

Keywords: Switched reluctance machines, Self-bearing machines, Modelling, Control, Finite element method

1. Introduction

Switched reluctance machines (SRMs) have a simple construction. The cross-sectional area of an 8/6 configuration is shown in Fig. 1. The rotor is made fully of soft magnetic material, e.g., of electrical steel sheets. The stator has eight teeth around which the stator armature winding is wound concentrically. The simple construction and inexpensive materials make switched reluctance machines a cost-effective choice.

In self-bearing machines, the stator armature winding or a separate levitation winding is used to produce radial force that supports the rotor instead of mechanical or separate active magnetic bearings. Without separate bearings the mass and length of the machine will be consequently reduced. The shaft length becomes shorter, which results in higher critical speeds and more stable operation (Chen and Hofmann, 2012). Typically, in self-bearing SRMs, there is an additional levitation winding in the stator for force production, and 12/8 configuration is used instead of 8/6 as for example in (Takemoto et al, 2001). Such configuration makes it easier to independently control the radial forces and torque, but however increases the number of phases and thus needed power electronics.

One self-bearing 8/6 SRM prototype has been developed in (Chen and Hofmann, 2007), (Chen and Hofmann, 2012). The stator currents are divided into three components. The radial forces and torque are approximated by polynomials as a function of the stator currents, rotor angle and position. In this way, PID controllers can be used for obtaining needed force and torque values from measured position and rotation speed, and for calculating the needed stator currents to produce the required forces. Compared to (Chen and Hofmann, 2007) and (Chen and Hofmann, 2012), we have placed our stator in a different position, as shown in Fig. 1. This does not affect the torque production, but has an impact on the radial forces, because the direction of the stator teeth is now different. Therefore, we have

implemented a different logic on how to switch on and off the eight stator coils. To our best knowledge, this switching logic of a self-bearing 8/6 SRM is new. The needed inverters and position estimation of this particular SRM has been previously discussed in (Haarnoja et al., 2014).

The modelling methods of SRM, with or without conventional mechanical bearings, have been broadly discussed in the literature. The typical methods include finite element method (FEM) (Li et al., 2009), reluctance networks (Deihimi et al., 2002), and other analytical methods such as (Stiebler and Liu, 1999). However the simple analytical models found in the literature are often developed for conventional SRMs with bearings, and do not take into account radial force production. Finite element method is accurate, but too slow for real-time control. Reluctance networks are also a possibility, but they are often laborious to implement and therefore not suitable for the control system.

Therefore we aim at developing a simplified analytical model for both radial forces and torque. The model has to be accurate enough to estimate the radial forces and torque based on rotor angle and stator currents, but simultaneously fast enough for control. The idea is to use piecewise defined polynomial functions for each switching period. The polynomials are fitted to data that have been obtained by electromagnetic finite element analysis. The results of the proposed simplified analytical model are be compared against FEM, and used to solve the required stator currents when the reference values for the radial forces and torque are known. The model can be used with closed loop control methods such as PID controllers to control both radial forces and torque of the SRM.

2. Modelling and Control of the Self-Bearing 8/6 SRM

The torque of the self-bearing 8/6 SRM is produced by exciting four opposite coils. When the absolute value of the current is same in all coils, the net radial force is zero. Nonzero net radial forces can be produced by increasing the current in two coils, which are chosen depending on the rotor angle, see Table 1. An example is shown in Fig. 1. The machine has eight independently controllable phases or coils. Four coils are excited simultaneously while others are switched off. The choice of the excited coils depends on the rotor angle θ_r. To simplify the control, the eight currents are represented by three components i_{f1}, i_{f2} and i_t. The actual coil currents $i_1 \dots i_8$ are calculated from the three components, based on the rotor angle. From the rotor angle, an angle for the stator teeth θ_s is obtained.

$$\theta_s = \begin{cases} 3(\theta_0 - \theta_r), & \theta_r \le \theta_0 \\ 3(60^\circ + \theta_0 - \theta_r), & \theta_r > \theta_0 \end{cases}, \tag{1}$$

where θ_0 is the initial angle of the rotor. Based on θ_s, the excited stator phases can be chosen as shown in Table 1.

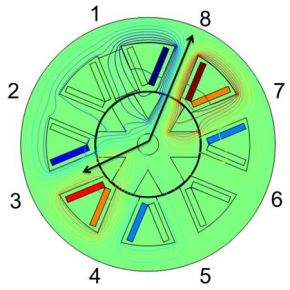

Fig. 1. Example of the control of the phase currents of the machine. In the depicted rotor position, radial forces can be produced by adding current to phases 3 and 8.

Table 1. Excitation of the stator phases in a period of 180°

θ_s (degrees)	i_t phase number	i_{f1} phase number	i_{f2} phase number
22.5-67.5	7,8,3,4	8	3
157.5-180 and 0-22.5	2,3,6,7	2	7
112.5-157.5	1,2,5,6	1	6
67.5-112.5	1,8,4,5	1	8

In order to be able to control a self-bearing SRM, an accurate but fast model is needed to calculate electromagnetic forces and torque. The task is challenging because of the non-linear characteristics of the SRM. To simplify the situation, we have assumed the machine is operated in unsaturated conditions, and that the rotor will stay close to the center point.

Our simplified analytical model is based on data that have been obtained with two-dimensional electromagnetic finite element analysis (COMSOL, Inc., 2016). The current densities in the coils are solved from the currents, numbers of winding turns in the coils and the cross-sectional area of the coil sides. In a static case, the magnetic field in the machine fulfills

$$\nabla \times \nu \nabla \times \boldsymbol{A} = \boldsymbol{J} \tag{2}$$

in which ν denotes the reluctivity, $\boldsymbol{A}$ the magnetic vector potential and $\boldsymbol{J}$ the current density.

The magnetic characteristics of the laminated cores are represented with a single-valued *BH*-curve that is shown in Fig. 2. The reluctivity of the air regions and coils is equal to that of free space.

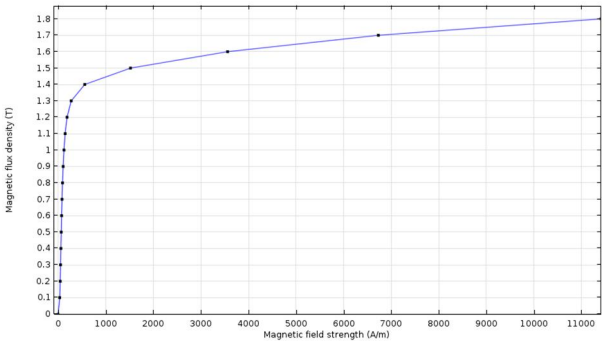

Fig. 2. *BH*-curve of the laminated soft magnetic cores.

The forces and torque can be obtained from the field solution by Maxwell stress tensor:

$$\boldsymbol{F} = \iint_S \mathrm{d}A(\overline{\boldsymbol{S}} \cdot \boldsymbol{n}) \tag{3}$$

$$\boldsymbol{\tau} = \iint_S \mathrm{d}A\boldsymbol{r} \times (\overline{\boldsymbol{S}} \cdot \boldsymbol{n}) \tag{4}$$

in which $\boldsymbol{F}$ denotes force vector, A the surface over which the Maxwell stress tensor is integrated, $\boldsymbol{n}$ normal vector of surface A, and $\boldsymbol{\tau}$ torque vector. Tensor $\overline{\boldsymbol{S}}$ is defined as

$$\overline{\boldsymbol{S}} = \frac{1}{\mu_0}\begin{bmatrix} B_x^2 - \frac{B^2}{2} & B_xB_y & B_xB_z \\ B_yB_x & B_y^2 - \frac{B^2}{2} & B_yB_z \\ B_zB_x & B_zB_y & B_z^2 - \frac{B^2}{2} \end{bmatrix} \tag{5}$$

in which B is the norm of magnetic flux density, i.e. $B = \sqrt{B_x^2 + B_y^2 + B_z^2}$.

Vector $\boldsymbol{r}$ is defined as

$$\boldsymbol{r} = (x - x_t)\boldsymbol{u}_x + (y - y_t)\boldsymbol{u}_y + (x - x_t)\boldsymbol{u}_z \tag{6}$$

in which point (x_t, y_t, z_t) is the torque origin.

Fig. 3 shows the magnetic flux density in the SRM with only torque production and with both radial force and torque production. These results have been obtained by exciting the coils 3, 4, 7 and 8 as shown in Fig. 1. If the amount of current supplied to the opposite coils is similar, the magnetic flux density is similar in both sides of the machine, and no radial forces will be produced. When the radial force producing currents are added, the magnetic flux density is increased in the uppermost and leftmost windings, causing nonzero net radial forces. By choosing the added currents

carefully, it is possible to generate a resultant force upwards.

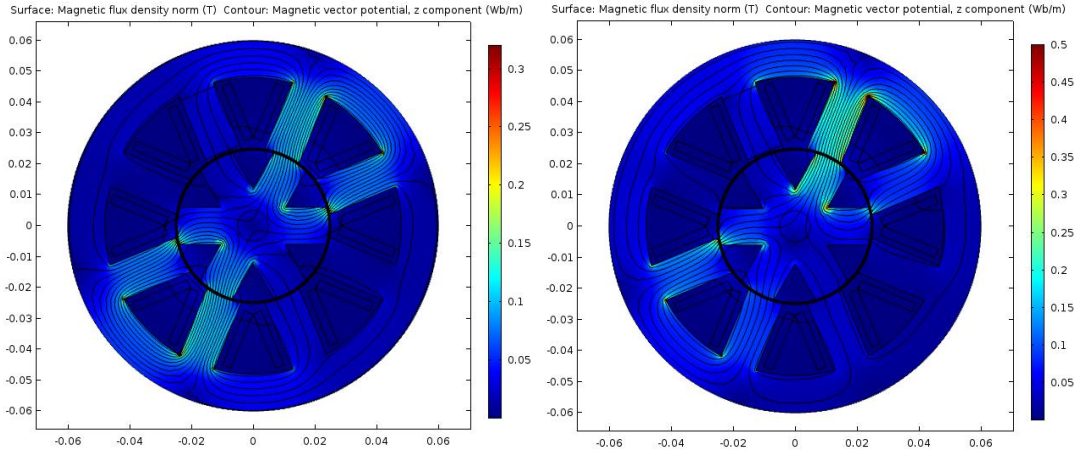

Fig. 3. Magnetic flux density in the proposed SRM under normal operation without the radial force production (left) and with both radial force and torque production (right).

The torque waveform is symmetric after 15 degrees, which means that the torque needs to be modelled during the first 15 degrees rotation only. The torque shape during one switching period is close to a polynomial function of degree 2, which is chosen for k_t.

$$T = k_t(\theta) i_t^2 \tag{7}$$

In order to obtain the simplified analytical model, a look-up-table (LUT) was computed solving the FE model with different rotor angles and stator current components i_t, i_{f1} and i_{f2}. The static FEM model has 56399 second order elements, and its computation time is 9 s. The LUT contains 4320 data points and the current values are from 0 to 3 A for each current component. The rotor angle is between 0° and 60°. A polynomial function was fitted to this data using the readily implemented functions in MATLAB's Curve Fitting Toolbox (The MathWorks, Inc., 2016). The rotor is assumed to stay in the center, so the effect of rotor movement is neglected at this point. The electromagnetic radial force then depends on the rotor angle and the current supplied to the stator winding. Because our current is rather low compared to the size of the machine, it is safe to assume that the iron is not saturated. According to FEM results, the magnetic flux density with $i_t = 8$ A was around 0.5 T in the teeth, as shown in Fig. 4.

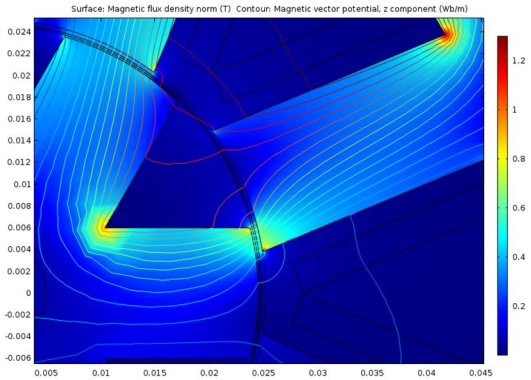

Fig. 4. Magnetic flux density in stator tooth and two rotor teeth when $i_t = 8$ A.

Therefore the force can be represented as

$$F(\theta_r, \boldsymbol{i}) = \boldsymbol{i}^T \boldsymbol{K}(\theta_r) \boldsymbol{i}, \tag{8}$$

where $\boldsymbol{i} = \begin{bmatrix} i_{f2} \\ i_{f1} \end{bmatrix}$ and $\boldsymbol{F} = \begin{bmatrix} F_x \\ F_y \end{bmatrix}$ and $\boldsymbol{K}(\theta_r) = \begin{bmatrix} k_{xx}(\theta_r) & k_{xy}(\theta_r) \\ k_{yx}(\theta_r) & k_{yy}(\theta_r) \end{bmatrix}$.

The coefficients on matrix $\boldsymbol{K}$ are functions of the rotor angle θ_r and are piecewise defined for the four switching periods. Based on FEM computations, a one degree polynomial function is used for each switching period. The

required current can be then solved from Eq. (8).

The cross-coupling between the radial force production and torque production has to be taken into account to control the motor properly. If the rotor is centered, the torque producing current i_t will not produce any radial force. However, the radial force producing currents will affect also the torque. Therefore the torque model has to be such that that it includes the effect of the currents i_{f1} and i_{f2}. The maximum effect is around 0.0012 Nm/A, and the values vary depending on the switching period. The proposed model is

$$T(\theta_r, i_t, i_{f1}, i_{f2}) = k_t(\theta_r)i_t^2 + k_{f1}(\theta_r)i_{f1}^2 + k_{f2}(\theta_r)i_{f2}^2 + k_{12}(\theta_r)i_{f1}i_{f2} + k_{t1}(\theta_r)i_t i_{f1} + k_{t2}(\theta_r)i_t i_{f2} \tag{9}$$

where $k_t(\theta_r)$ is the torque model as proposed in Eq. (7), and coefficients k are piecewise defined functions of the rotor angle θ_r.

The results of the proposed models are compared against the FE results in Fig. 5 and Fig. 6. The torque waveform agrees with the FE result, and the obtained values are close those obtained with FEM. The slight difference is probably due to the neglect of the saturation. Even though the motor is not saturated, it is typical for SRMs to have local saturation e.g. in the tooth tips, which can affect the forces. For radial forces, the results of the analytical model are also close to the FE results. However, there is some difference for rotor angles between 20° and 40° for the x-component of the forces and between 40° and 50° for the y-component of the force. This difference may cause some inaccuracy in the calculation of the current components. However, with proper control and high enough rotation speed, we presume that the effect of this possible inaccuracy on the performance of the machine is small enough.

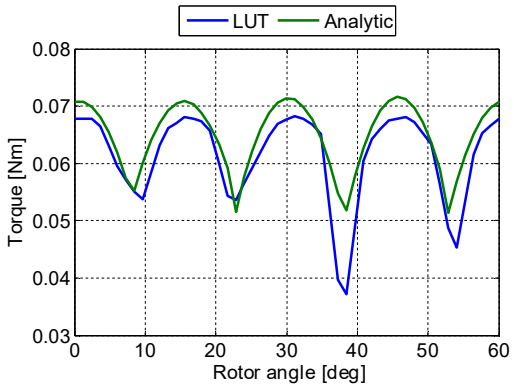

Fig. 5. Comparison between the analytical torque model, Eq. (9), and the LUT results. The currents are $i_{f1} = i_{f2} = 1$ A and $i_t = 3$ A. The green curve shows the torque given by the proposed model, and the blue curve is the torque obtained by using a look-up-table.

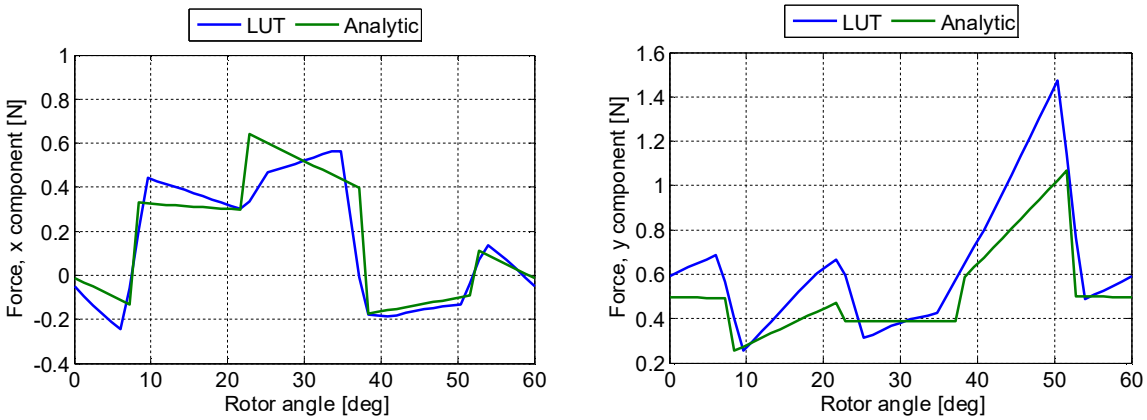

Fig. 6. Comparison between the analytical radial force model, Eq. (8), and the LUT results. The analytical model is capable of approximating the behavior of the radial forces in the self-bearing SRM.

Because we assume that the rotor stays in the center, we can assume that the torque producing current i_t does not produce radial forces. Therefore, we can now use the analytical Eq. (8) to solve first the currents i_{f1}, $i_{f2}$and after that

i_t, from Eq. (9), when the reference values for forces and torque are known.

3. Results

The torque model was tested with reference torque 0.02 Nm. The rotation was simulated over 60° and the current i_t was solved from Eq. (7), and the torque corresponding to the solved current was computed with the LUT. The results are shown in Fig. 7. The average torque is 0.0185 Nm, which corresponds to average error of 0.0015 Nm (7.42%) from the reference value. The error is partly due to the fact that correspondence between the simplified model and the data used for finding its polynomials was not perfect. Also the fact that saturation is not taken into account in the fitted polynomial functions, will cause some error. However, in the future our aim is to use PID controllers to control the rotation speed of the motor, and we assume that the use of PID controllers will smooth this error. The currents are between 1.85 A and 2.2 A. The current ripple has to be rather high in order to compensate the saliency.

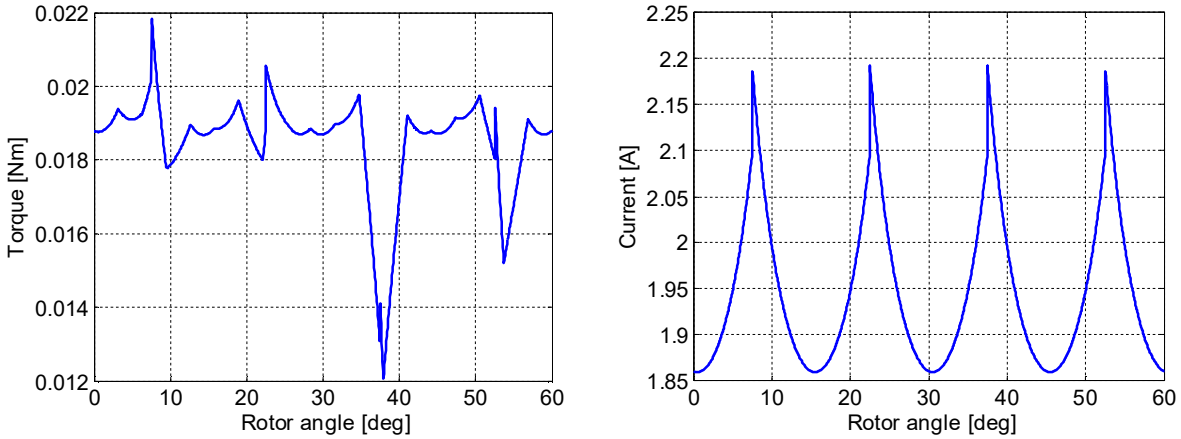

Fig. 7. The torque obtained with the LUT (left). The reference value for torque is 0.02 Nm. The required current obtained using the proposed torque model (Eq. (7)) i_t is shown on the right-hand side.

The forces are given reference values of 0 N in the *x*-direction and 5 N in the *y*-direction. The required currents are calculated using the proposed force model Eq. (8), and the motor is simulated over a 60 degree period to see how well the machine can be controlled with the model. The results are shown in Fig. 8. The average values are close to the given references, but the force ripple is high, as is typical for the motor type. The ripple results from the saliency of both stator and rotor.

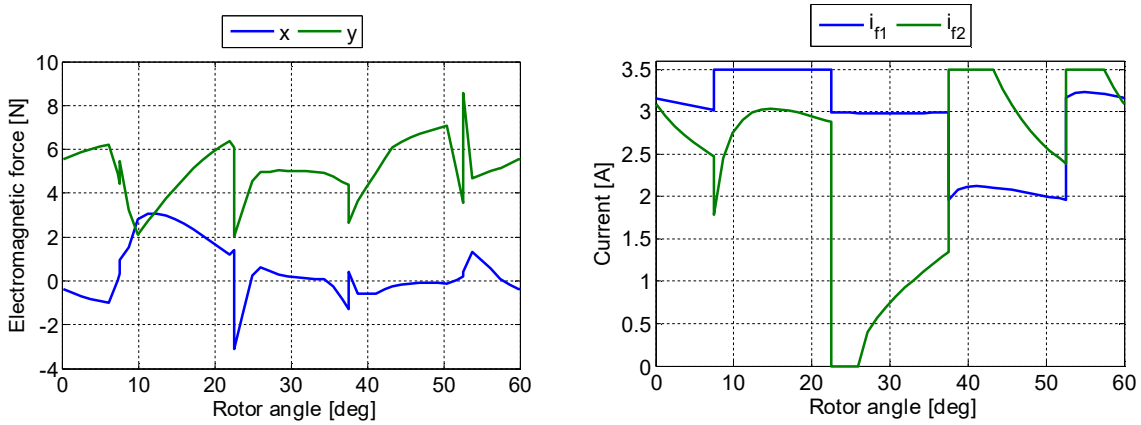

Fig. 8. Directly controlled forces over 60 degree period, with reference values $F_x = 0$ N and $F_y = 5$ N. The average values are $F_{x,ave} = 0.34$ N and $F_{y,ave} = 5.09$ N. The currents solved from Eq. (8) are shown on the right.

Figure 9 and Fig. 10 show the results of the system where both radial forces and torque are controlled directly with the model. The currents are again calculated over 60 degree period using Eq. (8) and Eq. (9). The maximum allowed current for the radial force production is 3.5 A. This limits the radial force production in some rotor angles, but not to

such extent that it would compromise the support of the rotor. The ripple in the radial forces is large. This is mainly because the radial force model is not perfectly accurate. It is worth noticing that in reality, there will be a PID controller added in the system, which will improve the performance. The torque production seems to work well as the torque follows the reference value quite well. The ripple is again due to the saliency of the rotor and stator, and also because of the fitted torque model is not perfectly accurate.

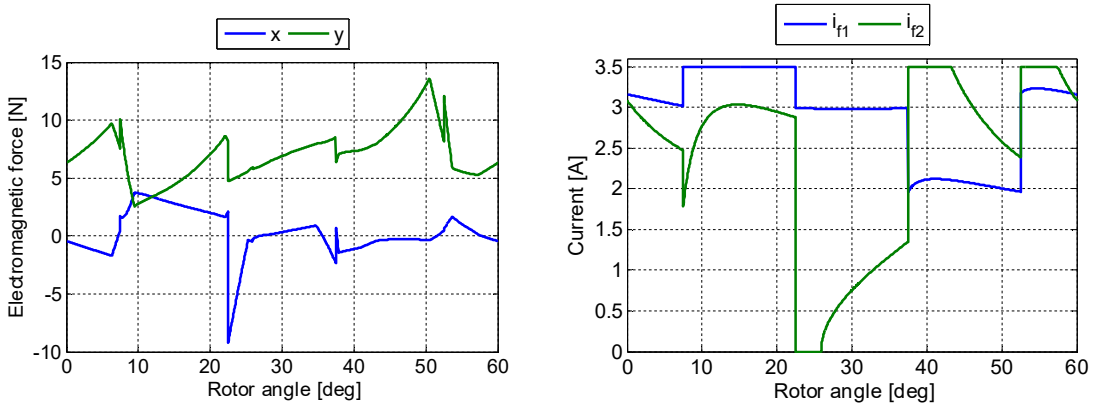

Fig. 9. Radial forces with torque production too, reference values are F_x = 0 N and F_y = 5 N (Left). Currents i_{f1} and i_{f2} (right) are obtained using Eq. (8) when the maximum allowed radial force current is 3.5 A.

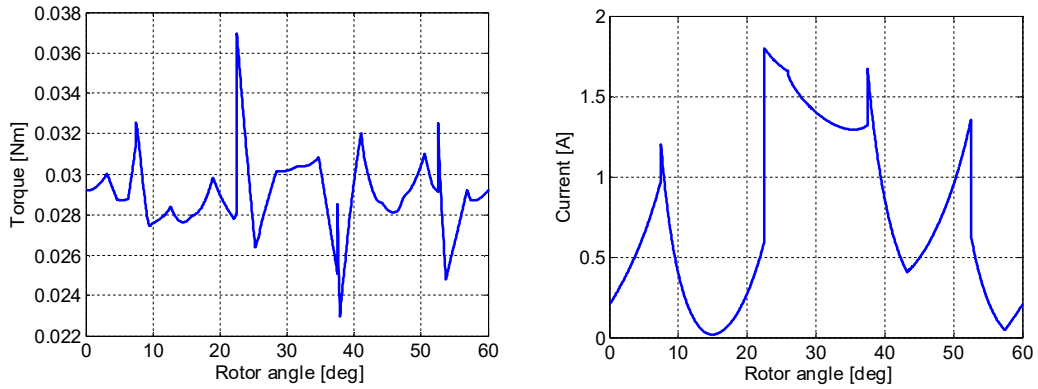

Fig. 10. Torque with radial force production, reference value is 0.03 Nm (left). The required current i_t (right) is solved from Eq. (9).

4. Discussion and Conclusions

A new switching logic for a self-bearing switched reluctance machine was presented, and a simplified analytical model for the torque and radial forces was proposed. The main idea is to use three current components and the rotor angle to obtain the stator currents in the eight independent phases. The analytical model is based on fitted polynomials and can be used in real time control to calculate the required stator current components. First, the results of the analytical model were compared against FE results, and the correspondence was found sufficient but not perfectly accurate.

The models were then tested using direct control so that the torque, and radial forces are given reference values, and the required stator currents were computed for different rotor angles. The results are that the torque control performs well, but in the radial force, there is quite a lot of ripple. However, the average value of the force is large enough to support the mass of the rotor. With closed loop control the performance will be improved. Thus the next task will be to design proper controllers for both radial forces and torque. Also probably at least in the radial force model, the rotor eccentricity should be taken into account to some extent. Possible methods to improve the analytical model would be to add a cross-coupling term also to the radial force model. At the moment it is not included, which may be one possible reason for the small inaccuracy in the forces.

The implemented switching logic works as was planned, and it is possible to obtain such currents at every rotor

angle that the machine works as was expected. However, it might be possible to reduce both torque and force ripple by developing the logic even further. For example, it might be worth trying to smooth the transition between two switching periods. In the future, the methods should also be tested in a laboratory in order to validate the proposed model and switching logic.

Acknowledgements

The authors wish to thank the Academy of Finland for funding this project.

References

Chen, L. and Hofmann, W., 2007, Performance Characteristics of one Novel Switched Reluctance Bearingless Motor Drive, Power Conversion Conference - Nagoya, 2007. PCC '07, Nagoya, 2007, pp. 608-613.

Chen, L. and Hofmann, W., 2012. Speed Regulation Technique of One Bearingless 8/6 Switched Reluctance Motor With Simpler Single Winding Structure, IEEE Transactions on Industrial Electronics, vol. 59, no. 6, pp. 2592-2600, June 2012.

COMSOL Inc., 2016. Comsol Multiphysics webpage. Available at: https://www.comsol.com/, accessed 16.5.2016.

Deihimi, A., Farhangi, S. and Henneberger, G., 2002. A general nonlinear model of switched reluctance motor with mutual coupling and multiphase excitation., Electrical Engineering, Vol. 84, no. 3, pp 143-158.

Haarnoja, T., Halmeaho, T., Manninen, A. and Tammi, K., 2014., Position estimation method for self-sensing electric machines based on the direct measurement of the current slope, Power Electronics, Machines and Drives (PEMD 2014), 7th IET International Conference on, Manchester, 2014, pp. 1-6.

Li, J., Choi, D. and Cho, Y., 2009, Analysis of Rotor Eccentricity in Switched Reluctance Motor With Parallel Winding Using FEM, IEEE Transactions on Magnetics, vol. 45, no. 6, pp. 2851-2854, June 2009.

Stiebler, M. and Liu, K., 1999, An analytical model of switched reluctance machines, in IEEE Transactions on Energy Conversion, vol. 14, no. 4, pp. 1100-1107, Dec 1999.

Takemoto M., Suzuki, H., Chiba, A., Fukao, T., and Rahman, M. A., 2001, Improved analysis of a bearingless switched reluctance motor, IEEE Transactions on Industry Applications, vol. 37, no. 1, pp. 26-34, Jan/Feb 2001.

The MathWorks, Inc., 2016. MATLAB Curve Fitting Tool web page,
Available at: http://se.mathworks.com/products/curvefitting/index.html?s_tid=gn_loc_drop, accessed 18.5.2016.